MULTI-OBJECTIVE DESIGN OPTIMIZATION OF BRUSHLESS DC AND SYNCHRONOUS RELUCTANCE MOTORS FOR LIGHT ELECTRIC VEHICLE APPLICATIONS

ANURAG SHARMA



DEPARTMENT OF ELECTRICAL ENGINEERING
INDIAN INSTITUTE OF TECHNOLOGY DELHI
JULY 2026

© Indian Institute of Technology Delhi (IITD), New Delhi, 2026

Multi-Objective Design Optimization of Brushless DC and Synchronous Reluctance Motors for Light Electric Vehicle Applications

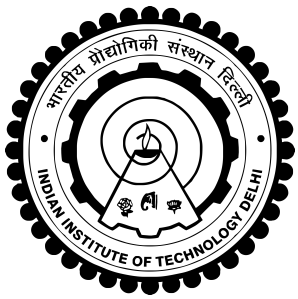
by

Anurag Sharma
Department of Electrical Engineering

Submitted

in fulfilment of the requirements of the degree of

Doctor of Philosophy



INDIAN INSTITUTE OF TECHNOLOGY DELHI
July 2026

dedicated to my parents, sister, wife and son...

Certificate

This is to certify that the thesis titled **"MULTI-OBJECTIVE DESIGN OPTIMIZATION OF BRUSHLESS DC AND SYNCHRONOUS RELUCTANCE MOTORS FOR LIGHT ELECTRIC VEHICLE APPLICATIONS"**, submitted by **Anurag Sharma, 2018EEZ8556**, to the Indian Institute of Technology, Delhi, for the award of the degree of **Doctor of Philosophy**, is a bonafide record of the research work done by him under my supervision. The contents of this thesis, in full or in parts, have not been submitted to any other Institute or University for the award of any degree or diploma.

Dr. Amit Kumar Jain
Professor,
Dept. of Electrical Engineering,
Indian Institute of Technology, Delhi, 110 016.

Acknowledgements

I would like to express my heartfelt gratitude to my PhD supervisor, Prof. Amit Kumar Jain, for his invaluable guidance and support throughout my research. His expertise, constructive feedback, and encouragement were crucial at every stage of my PhD journey, directly contributing to the completion of this thesis. He provided clear and practical suggestions, allowing me to explore my interests and work with independence. I am truly thankful for his trust and guidance, both professionally and personally, and will always value the lessons I learned under his supervision.

I am also deeply thankful to my Student Research Committee members, Prof. Anandarup Das, Prof. Soumya Shubhra Nag, and Prof. Sumit K. Chattopadhyay, for their encouragement, progress monitoring, and valuable suggestions throughout my PhD journey. Their constructive feedback and observations at different stages helped me stay on track and enhance the quality of my research work. My sincere appreciation also goes to Prof. Ramkrishan Maheshwari and Prof. Sumit Pramanick for their teachings and mentorship during the early phases of my PhD, which helped me build a strong technical foundation.

I would like to thank my lab mates, seniors, and fellow Phd students, Dr. Durgesh Kumar Banchorr, Vaibhav Bhardwaj, Sagar Gupta, Abhishek Shaw, Sumit Kumar Singh, Dr. Himanshu Swami, Dr. Rahul Sharma, Dr. Nidhi Bisht, Dr. Prasun Mishra, Dr. Manish Kumar, Dr. Debi Prasad Nayak, Dr. Yakala Ravi Kumar, Dr. Apurva Verma, Dr. Suvom Roy, Arkabrata Dattaroy, Vaibhav Vijaykumar Fere, Ruttala Sankarrao, Dr. Rohit Kumar, Dr. Vipin Kumar Singh, Dr. Sukrashis Sarkar, Dr. Subhasis Nayak, for their support, cooperation, discussions, and friendly help whenever needed.

I would also like to acknowledge the support received from the industry during different phases of my PhD work. I am thankful to industry leaders Mr. Narayanaswamy Ramakrishnan (then GM R&D, Luminous Power Technologies Pvt Ltd), Mr. Rakesh Malhotra (Founder, SAR group), and Mr. Akashdeep Singh (Founder, Calvem Energy Pvt Ltd) for their support in various forms. Their encouragement and industry perspective were instrumental in taking the research closer to practical implementation. A special mention to Calvem Energy Pvt Ltd for supporting in prototype realization in this thesis.

I express my deepest gratitude to my parents, sister, and wife for their unconditional support and belief in me. Their sacrifices, patience, encouragement, and constant faith have been the real strength behind this journey. Without their support, completing this work would not have been possible. I am also thankful to my son, Madhav, for bringing joy to my life.

Finally, I thank the Almighty for the divine guidance that has kept me strong and hopeful throughout my PhD journey.

Anurag Sharma

Abstract

Electric Vehicles (EVs) are increasingly being adopted as a practical solution to mitigate air pollution. Within this transition, Light Electric Vehicles (LEVs), which include e-rickshaws and L5 category three-wheeled e-loaders, have become essential for last-mile connectivity in India. The traction motor is the primary determinant of vehicle performance because it directly influences the energy efficiency, reliability, and overall cost. Motivated by these considerations, this thesis addresses two independent research problems relevant to LEVs.

The thesis first deals with the design, development, and testing of a square-wave-driven Interior Permanent Magnet (IPM) Brushless DC (BLDC) motor. The motivation is to develop a cost-effective alternative to the commercially available Surface Permanent Magnet (SPM) BLDC motor for the e-rickshaw application. A key challenge associated with square-wave-driven IPM-BLDC motors is addressed, which is the degradation of average torque at high speeds due to high winding inductance. To solve this issue, trapezoidal notches are introduced on the quadrature axis of the rotor to reduce inductance and enhance high-speed torque capability. The proposed motor is optimized using Non-dominated Sorting Genetic Algorithm II (NSGA-II) applied on the Support Vector Regression (SVR) surrogate model. The reliability and practicality of the proposed motor are evaluated through thermal, demagnetization, and rotor stress analyses. Additionally, commercial viability is assessed through the cost analysis of the motor. Finally, a 1 kW prototype of the motor is fabricated and validated in lab and field trials.

The second study focuses on traction motor design for L5 category three-wheeled e-loaders, which predominantly use rare-earth elements-based Permanent Magnet Synchronous Motors (PMSMs). Owing to their reliance on rare-earth magnets, these motors have an environmental impact and are subject to supply chain risks driven by geopolitical factors. As a rare-earth-free alternative, the Synchronous Reluctance Motor (SynRM) is investigated; however, its design is challenging due to the large number of rotor design parameters. A curved-barrier SynRM motor topology is developed and optimized to meet the performance targets. The main highlight of the study is the proposed online surrogate-assisted multi-objective op-

timization framework with adaptive infill sampling. This approach significantly reduces computational time, i.e., the number of Finite Element Analysis (FEA) runs, while achieving design solutions comparable to those of a conventional optimization approach. The study also includes optimization results using conventional optimization approaches for a fair comparison. Experimental results are included to validate the electromagnetic FEA modeling.

Overall, this thesis contributes: (i) two improved traction motor solutions aligned with the LEV requirements, and (ii) a computationally efficient online surrogate-assisted multi-objective optimization framework that may be beneficial for high-dimensional electric machine design problems.

सार

वायु प्रदूषण को कम करने के लिए इलेक्ट्रिक वाहनों (EVs) को एक व्यावहारिक समाधान के तौर पर तेज़ी से अपनाया जा रहा है। इस बदलाव के दौर में, भारत में 'लास्ट-माइल कनेक्टिविटी' (यानी यात्रा के आखिरी चरण की कनेक्टिविटी) के लिए लाइट इलेक्ट्रिक वाहन (LEVs) बहुत ज़रूरी हो गए हैं; इनमें ई-रिक्शा और L5 कैटेगरी के तीन-पहिया ई-लोडर शामिल हैं। ट्रैक्शन मोटर वाहन की परफॉर्मेंस तय करने वाला मुख्य हिस्सा है क्योंकि यह सीधे तौर पर ऊर्जा दक्षता, विश्वसनीयता और कुल लागत पर असर डालती है। इन्हीं बातों को ध्यान में रखते हुए, यह थीसिस LEVs से जुड़ी दो अलग-अलग रिसर्च समस्याओं पर चर्चा करती है।

यह थीसिस सबसे पहले स्क्वायर-वेव से चलने वाली इंटीरियर परमानेंट मैग्नेट (IPM) ब्रशलेस DC (BLDC) मोटर के डिज़ाइन, डेवलपमेंट और टेस्टिंग पर बात करती है। इसका मकसद ई-रिक्शा के लिए कम कीमत वाला ऐसा विकल्प बनाना है जो बाज़ार में मिलने वाली सरफेस परमानेंट मैग्नेट (SPM) BLDC मोटर की जगह ले सके। इसमें स्क्वायर-वेव से चलने वाली IPM-BLDC मोटर से जुड़ी एक मुख्य चुनौती को हल किया गया है: हाई स्पीड पर ज़्यादा वाइंडिंग इंडक्टेंस के कारण औसत टॉर्क का कम हो जाना। इस समस्या को हल करने के लिए, इंडक्टेंस को कम करने और हाई-स्पीड टॉर्क क्षमता को बढ़ाने के लिए रोटर के क्वाड्रैचर एक्सिस पर ट्रेपेज़ॉइडल नॉच बनाए गए हैं। प्रस्तावित मोटर को सपोर्ट वेक्टर रिग्रेशन (SVR) सरोगेट मॉडल पर नॉन-डोमिनेटेड सॉर्टिंग जेनेटिक एल्गोरिदम II (NSGA-II) का इस्तेमाल करके ऑप्टिमाइज़ किया गया है। थर्मल, डीमैग्नेटाइज़ेशन और रोटर स्ट्रेस एनालिसिस के ज़रिए प्रस्तावित मोटर की विश्वसनीयता और व्यावहारिकता का मूल्यांकन किया गया है। इसके अलावा, मोटर की लागत का विश्लेषण करके इसकी व्यावसायिक व्यवहार्यता का भी आकलन किया गया है। आखिर में, मोटर का 1 kW का प्रोटोटाइप बनाया गया है और लैब व फील्ड ट्रायल में इसे वैलिडेट किया गया है।

दूसरी स्टडी L5 कैटेगरी के तीन-पहिया ई-लोडर्स के लिए ट्रैक्शन मोटर डिज़ाइन पर केंद्रित है, जिनमें ज़्यादातर रेयर-अर्थ एलिमेंट पर आधारित परमानेंट मैग्नेट सिंक्रोनस मोटर्स (PMSMs) का इस्तेमाल होता है। रेयर-अर्थ मैग्नेट पर निर्भरता के कारण, इन मोटरों का पर्यावरण पर असर पड़ता है और जियोपॉलिटिकल वजहों से इनकी सप्लाई चेन में जोखिम रहता है। रेयर-अर्थ-फ्री विकल्प के तौर पर, सिंक्रोनस रिलक्टेंस मोटर (SynRM) की जांच की गई है; हालाँकि, रोटर डिज़ाइन पैरामीटर्स की बड़ी संख्या के कारण इसका डिज़ाइन चुनौतीपूर्ण है। परफ़ॉर्मेंस लक्ष्यों को पूरा करने के लिए एक कर्व्ड-बैरियर SynRM मोटर टोपोलॉजी विकसित और ऑप्टिमाइज़ की गई है। इस स्टडी की मुख्य विशेषता एडेप्टिव इनफ़िल सैंपलिंग के साथ प्रस्तावित ऑनलाइन सरोगेट-असिस्टेड मल्टी-ऑब्जेक्टिव ऑप्टिमाइज़ेशन फ़्रेमवर्क है। यह तरीका कंप्यूटेशनल समय, यानी फ़ाइनाइट एलिमेंट एनालिसिस (FEA) रन की संख्या को काफ़ी कम करता है, साथ ही पारंपरिक ऑप्टिमाइज़ेशन तरीके के बराबर डिज़ाइन समाधान भी देता है। स्टडी में सही तुलना के लिए पारंपरिक ऑप्टिमाइज़ेशन तरीकों का इस्तेमाल करके ऑप्टिमाइज़ेशन के

नतीजे भी शामिल हैं। इलेक्ट्रोमैग्नेटिक FEA मॉडलिंग को वेरिफ़ाई करने के लिए एक्सपेरिमेंटल नतीजे भी शामिल किए गए हैं।

कुल मिलाकर, यह थीसिस इन चीज़ों में योगदान देती है: (i) LEV की ज़रूरतों के हिसाब से ट्रैक्शन मोटर के दो बेहतर समाधान, और (ii) एक कंप्यूटेशन के लिहाज़ से कुशल ऑनलाइन सरोगेट-असिस्टेड मल्टी-ऑब्जेक्टिव ऑप्टिमाइज़ेशन फ़्रेमवर्क, जो ज़्यादा डाइमेंशन वाली इलेक्ट्रिक मशीन डिज़ाइन की समस्याओं के लिए फ़ायदेमंद हो सकता है।

Table of Contents

Certificate **i**

Acknowledgements **ii**

Abstract **iv**

List of Figures **x**

List of Tables **xv**

Acronyms **xvii**

Notation **xviii**

1 Introduction **1**

1.1 Background 2

1.2 Motivation and Research Problems 5

1.2.1 Research problem 1 5

1.2.2 Research problem 2 6

1.3 Outline of the Thesis 9

2 Multi-Objective Optimization of Interior Permanent Magnet Brushless DC Motor for e-Rickshaws **12**

2.1 General 13

2.2 Review of Brushless DC Motor 14

2.3 Current State of the Art 16

2.4 Application Overview and Specifications 18

2.5 Brushless DC Motor with Conventional IPM Rotor 19

2.5.1 Torque Degradation in High-Speed Regions 21

2.6 Brushless DC Motor with Proposed IPM Rotor 23
2.6.1 Proposed IPM Rotor 23
2.6.2 Analytical Model of the Proposed Rotor 24
2.6.2.1 Back EMF 26
2.6.2.2 Winding Inductance 26
2.6.2.3 Expressions of Fourier Coefficients 27
2.6.3 Effect of notch parameters on Back EMF and winding inductance 28
2.7 FE Analysis of Proposed, Conventional and Benchmark Motors . 28
2.8 Multi-Objective Optimization of the Proposed IPM-BLDC Motor 33
2.9 FE Analysis of Initial and Optimal Designs of Proposed Motor . . 38
2.10 Reliability and Cost Assessment of the Proposed Motor 42
2.10.1 Thermal Analysis 42
2.10.2 Demagnetization Analysis 44
2.10.3 Rotor Stress Analysis 46
2.10.4 Cost Analysis 46
2.10.4.1 Process and assembly costs 47
2.10.4.2 Tooling costs 47
2.11 Prototype Development and Lab Validation of the Proposed Motor 49
2.12 Chapter Summary 53

3 Multi-Objective Optimization of Synchronous Reluctance Motor for Electric Three Wheelers 54

3.1 General 55

Part A: Literature Review and Initial Design of Synchronous Reluctance Motor

3.2 Review of Synchronous Reluctance Motor 57
3.3 Review of Data-Driven Surrogate Models for Multi-Objective Optimization 62
3.4 Current State of the Art 64
3.5 Application Overview and Specifications 69
3.6 Initial Design of Synchronous Reluctance Motor 70

3.6.1 Rotor Geometry Parametrization for SynRM 70
3.6.2 Design Overview 73
3.6.3 FEA Comparison of Segmented and Curved Barriers Rotor Design based SynRM 74

Part B: Multi-Objective Optimization of Synchronous Reluctance Motor

3.7 Problem Formulation and Introduction to Surrogate Assisted Optimization 79
3.8 Development of Offline Surrogate Assisted Optimization 83
3.8.1 Initial Dataset 83
3.8.2 Surrogate Model Development 86
3.8.3 Multi-Objective Optimization using NSGA-II 98
3.9 Development of Online Surrogate Assisted Optimization 100
3.9.1 Preliminaries 102
3.9.1.1 Gaussian Process Regression 102
3.9.1.2 Hypervolume improvement 105
3.9.1.3 Probability of Feasibility (POF) 106
3.9.2 Implementation of Method 108
3.9.3 Optimization Results 115
3.10 Discussion 119

Part C: Comparative Assessment of the Optimal SynRM Design

3.11 Performance Evaluation of Initial and Optimal SynRM 121
3.12 Thermal and Mechanical Stress Analysis of the Optimal SynRM . 126
3.13 Experimental Validation of the FEA Modeling 127
3.13.1 Reference SynRM Design 127
3.13.2 Experimental Setup 130
3.13.3 Experimental Results and FEA Comparison 131
3.14 Chapter Summary 134

4 Conclusion and Future Work 136

4.1 Conclusion 136
4.2 Future Outlook 137

A Supplementary Material for Chapter 2 **138**

B Supplementary Material for Chapter 3 **140**

C Supporting Concepts and Mathematical Definitions **141**

Bibliography **150**

Research Outcomes **169**

Author's Bio **170**

List of Figures

1.1 Electric vehicle penetration data, i.e., EV growth out of overall automotive sales, of the last three financial years. 3

1.2 Radar chart comparison of EV traction motor topologies (IPMSM, SynRM, IM, SRM) across key performance and implementation criteria. Radial extent denotes relative merit (higher score is better). 7

2.1 (a) BLDC motor drive scheme. (b) Equivalent circuit. 15

2.2 Illustration of motor dimensions. (a) Conventional IPM rotor. (b) Stator. 20

2.3 Conventional IPM-BLDCM characteristics compared with benchmark motor on a square-wave drive. (a) Torque versus Speed. (b) Current versus Speed. 22

2.4 (a) Major dimensions of the Proposed IPM rotor. (b) A 3-D cut section view of the proposed motor highlighting the rotor geometry. 23

2.5 Various notch geometries. (a) Circular. (b) Rectangular. (c) Trapezoid. 24

2.6 Leakage flux depiction through outer ribs. (a) Trapezoidal Notch. (b) Circular Notch. 24

2.7 Flux lines distribution. (a) Due to the rotor notch. (b) At the stator slot. 25

2.8 Effect of notch parameters on back EMF e_{ph} and phase inductance L_s. 28

2.9 Comparison of airgap flux density and back EMF along with the respective harmonics for benchmark, conventional, and proposed motor. (a) Airgap flux density. (b) Airgap harmonics. (c) Open circuit back EMF. (d) Harmonics in back EMF. 29

2.10 Winding self-inductance of proposed IPM-BLDC motor compared with benchmark and conventional motors. 30

2.11 Cogging torque of proposed IPM-BLDC motor compared with benchmark and conventional motors. 30

2.12 On-load performance comparison of proposed motor with benchmark and conventional motors at peak and rated conditions. (a) Peak torque at 350 RPM. (b) Peak current at 350 RPM. (c) Rated torque at 2800 RPM. (d) Rated current at 2800 RPM. 32

2.13 Workflow for the design optimization using NSGA-II optimization algorithm. 33

2.14 Spearman's rank correlation coefficient of objective functions f_1, f_2 and f_3. 35

2.15 Comparison of SVR surrogate predicted results with FEA results for the 20 random datasets for the objective functions f_1, f_2, and f_3. 36

2.16 Multi-objective optimization results using the Non Dominated Sorting Genetic Algorithm-II (NSGA-II). (a) Non-dominated solutions (Pareto optimal points) after 200 generations, with the selected design highlighted. (b) Generation-wise trend of the Best fitness of f_1 (N·m), f_2 (N·m), and f_3 (%). (c) Generation-wise trend of the average values of notch depth h_n and ratio β. 37

2.17 Initial and optimal rotor geometry. 38

2.18 Comparison of airgap flux density and back EMF along with the respective harmonics for initial and optimal design of proposed IPM-BLDC Motor. (a) Airgap flux density. (b) Airgap harmonics. (c) Open circuit back EMF. (d) Harmonics in back EMF. 40

2.19 Winding self-inductance of optimally designed proposed IPM-BLDC motor post multi-objective optimization using NSGA-II algorithm compared with the initial design of the proposed IPM-BLDC motor. 41

2.20 Cogging torque of optimally designed proposed IPM-BLDC motor post multi-objective optimization using NSGA-II algorithm compared with the initial design of the proposed IPM-BLDC motor. 41

2.21 On-load performance comparison of optimally designed proposed IPM-BLDC motor post multi-objective optimization using NSGA-II algorithm with the initial design of the proposed IPM-BLDC motor. (a) Peak torque at 350 RPM. (b) Rated torque at 2800 RPM. 42

2.22 Characteristics comparison of all Brushless DC motor designs. (a) Torque-speed characteristics. (b) Current-speed characteristics. . . 43

2.23 Thermal analysis of the optimal design of the proposed IPM-BLDC motor and comparison with the benchmark motor under the same operating conditions. (a) Temperature rise of components at 350 RPM and 150 A phase current. (b) Temperature rise of components at 2800 RPM and 22 A phase current. 44

2.24 PM demagnetization risk comparison at 115°C magnet temperature and 150 A phase current. (a) Benchmark PM remanent flux density B_{rem}. (b) Proposed PM remanent flux density B_{rem}. 45

2.25 Mechanical stress distribution of optimal rotor geometry (in MPa). 45

2.26 Various prototyping stages of the proposed IPM-BLDC motor. (a) Single rotor lamination. (b) Rotor stack. (c) Semi-assembled view. (d) Finished motor. 48

2.27 Experimental Test Setup. 48

2.28 Open circuit Line-Line back EMF measurement of proposed IPM-BLDC motor prototype (optimal design) and benchmark motor at 2800 RPM. 49

2.29 Phase current waveform captured in On-load testing of proposed IPM-BLDC motor prototype (optimal design) and benchmark motor at rated speed of 2800 RPM. 49

2.30 Performance characteristics comparison of proposed IPM-BLDC motor prototype (optimal design) and benchmark motor. (a) Torque versus speed. (b) Mechanical power versus speed. (c) Phase current versus speed. 51

2.30 Performance characteristics comparison of proposed IPM-BLDC motor prototype (optimal design) and benchmark motor (continued). (d) Motor efficiency versus speed. 52

2.31 Vehicle-level testing of the proposed IPM-BLDC motor prototype. Each snapshot is hyperlinked to the test video: `https://www.youtube.com/shorts/KKY3YkuVxaE`. 52

3.1 SynRM rotor major design parameters. 71

3.2 Generalized kth rotor barrier representation. 72

3.3 (a) Torque versus speed characteristics with WLTP Class-1 drive-cycle points corresponding to L5N category Electric three-wheeler loader. (b) Variation of phase current I_{pk}, current phase angle (β), and saliency ratio with speed. (c) Electromagnetic peak torque T_{pk} with respect to rotor position. 76

3.4 (a) Torque, mechanical power, and speed profiles corresponding to the WLTP driving cycle. (b) Motor drive-cycle efficiency. 78

3.5 Pairwise scatter matrix of the 18 design variables (x_1, x_2, $\cdots$, x_{18}) generated using Latin Hypercube Sampling (LHS), with marginal histograms on the diagonal. 85

3.6 Statistical distribution of the DOE responses. (a) Histogram and (c) Box plot of average torque T_{pk} (N·m). (b) Histogram and (d) Box plot of torque ripple TR_{pk} (%). 86

3.7 Prediction accuracy (on test set) for average torque T_{pk} using GPR, SVR, and ANN surrogate models trained with sample sizes $n = \{1000, 2000, 3000, 5000, 8000\}$. (a) Coefficient of determination (R^2) versus training sample size. (b) Root mean square error (RMSE) versus training sample size. 89

3.8 Prediction accuracy (on test set) for torque ripple TR_{pk} using GPR, SVR, and ANN surrogate models trained with sample sizes $n = \{1000, 2000, 3000, 5000, 8000\}$: (a) Coefficient of determination (R^2) versus training sample size; (b) Root mean square error (RMSE) versus training sample size. (c) Total training time (torque + torque ripple) for GPR, SVR, and ANN versus training sample size. . . . 90

3.9 Parity and box plots comparison for GPR, SVR, and ANN for T_{pk} and TR_{pk} trained on DOE size n of **1000**. (a)-(c) Parity plot comparison of GPR, SVR, and ANN for T_{pk}. (d) Box plot comparison of GPR, SVR, and ANN for T_{pk}. (e)-(g) Parity plot comparison of GPR, SVR, and ANN for TR_{pk}. (h) Box plot comparison of GPR, SVR, and ANN for TR_{pk}. 95

3.10 Parity and box plots comparison for GPR, SVR, and ANN for T_{pk} and TR_{pk} trained on DOE size n of **3000**. (a)-(c) Parity plot comparison of GPR, SVR, and ANN for T_{pk}. (d) Box plot comparison of GPR, SVR, and ANN for T_{pk}. (e)-(g) Parity plot comparison of GPR, SVR, and ANN for TR_{pk}. (h) Box plot comparison of GPR, SVR, and ANN for TR_{pk}. 96

3.11 Parity and box plots comparison for GPR, SVR, and ANN for T_{pk} and TR_{pk} trained on DOE size n of **8000**. (a)-(c) Parity plot comparison of GPR, SVR, and ANN for T_{pk}. (d) Box plot comparison of GPR, SVR, and ANN for T_{pk}. (e)-(g) Parity plot comparison of GPR, SVR, and ANN for TR_{pk}. (h) Box plot comparison of GPR, SVR, and ANN for TR_{pk}. 97

3.12 Non-dominated solutions (Pareto front) obtained using the NSGA-II algorithm. The selected design is highlighted in a black square box. 98

3.13 Posterior Gaussian Process Model distribution for a 1-D example. 104

3.14 Illustration of the hypervolume and hypervolume improvement for a bi-objective minimization problem. The non-dominated points $\mathbf{f}^{(1)}$, $\mathbf{f}^{(2)}$, $\mathbf{f}^{(3)}$, $\mathbf{f}^{(4)}$ form the current Pareto front, $\mathbf{r}$ denotes the reference point and $\mathbf{y}$ denotes new point. 105

3.15 Workflow of online surrogate-assisted NSGA-II optimization with infill sampling. 109

3.16 Iteration-wise progress [$iter$5-10] of the Pareto front in online surrogate-assisted optimization. 116

3.17 Iteration-wise progress of true Pareto front. (a) Growth of hypervolume. (b) Growth of the true Pareto front count. 118

3.18 Predicted and true Pareto fronts obtained in 10^{th} iteration of online surrogate-assisted optimization compared with Pareto fronts obtained by conventional offline surrogate-assisted and direct FEA optimization. 119

3.19 A visual comparison of rotor barriers (single pole) of optimal and initial SynRM designs. Optimal design is shown in blue color, whereas black (dashed) lines show the initial design. 122

3.20 Torque versus speed characteristics (optimal design versus initial design) with WLTP Class-1 drive-cycle points corresponding to L5N category Electric three-wheeler loader. 124

3.21 Temperature variation of different motor parts over the drive cycle. 126

3.22 Von Mises Stress analysis of the optimal rotor design. 127

3.23 (a) Test setup [Test video: https://youtu.be/XFw8y18CQCo]. (b) Fabricated SynRM prototype. 131

3.24 Implementation of the field-oriented control architecture of the SynRM drive. 132

3.25 Measured and FEA-predicted torque variation with current angle (β) at a phase current of 122 A. 132

3.26 3-phase analyzer screenshots of meter readings and phase currents for SynRM under test. (a)-(b) Rated condition. (c)-(d) Peak current condition. 133

A.1 Non-dominated solutions obtained from NSGA-II for conventional IPM-BLDC motor. 138

A.2 Dimensions of 12 slots 8-pole benchmark SPM-BLDC motor. (a) Stack length. (b) Stator outer diameter. 139

B.1 (a) Major dimensions of 36 slots 8 pole benchmark IPMS motor (in mm). (b) Disassembled rotor hardware. 140

C.1 Gaussian distribution function. 145

List of Tables

2.1 Current state of the art in IPM rotor based motor designs with notches 17

2.2 e-Rickshaw vehicle and traction motor specifications 19

2.3 Stator design parameters which are kept fixed throughout the optimization process 21

2.4 Performance parameters comparison 31

2.5 Main design variables for the proposed motor 34

2.6 Optimization results comparing initial and optimal designs 39

2.7 Cost of materials (in USD) 46

2.8 Experimental results at rated condition 50

3.1 Current state of the art in design optimization of Synchronous Reluctance Motor 66

3.2 Vehicle model of L5 category e-loader 69

3.3 Traction motor specifications for L5 category e-loaders 70

3.4 Fixed design parameters of Synchronous Reluctance Motor 73

3.5 Initial SynRM rotor design parameters 74

3.6 Performance comparison of initial SynRM design with segmented and curved rotor barriers at peak and continuous operation 75

3.7 Design variables and their bounds used in the Optimization process ($x_1 - x_{16}$ are geometric design variables to set the rotor barriers and carriers, x_{17} is the stack length, and x_{18} is the peak phase current.) 80

3.8 Statistical summary of the design variables in the initial dataset $\mathbf{X}$ 84

3.9 Error metrics (with respect to FEA) for GPR, SVR, and ANN trained across dataset sizes $n = \{1000, 2000, 3000, 5000, 8000\}$ 93

3.10 Error metrics of average torque T_{pk} and torque ripple TR_{pk} (FEA - Predicted) of the corresponding Pareto points obtained via NSGA-II optimization on ANN-based surrogate model trained with different training dataset sizes 99

3.11 Comparison of direct FEA, offline surrogate-assisted, and online surrogate-assisted optimization outcomes 120

3.12 Comparison of initial and optimal rotor design parameters 121

3.13 Performance Comparison of initial and optimal designs 123

3.14 A perspective comparison of the optimal SynRM design with other studies (B/M is IPMSM) 125

3.15 Reference SynRM major parameters compared with the optimal SynRM 128

3.16 Comparison of reference and optimal SynRM rotor design parameters 128

3.17 FEA comparison of reference and optimal SynRM designs 129

Acronyms

EV	Electric Vehicle
LEV	Light Electric Vehicle
ICE	Internal Combustion Engine
PM	Permanent Magnet
BLDC	Brushless DC Motor
PMSM	Permanent Magnet Synchronous Motor
SynRM	Synchronous Reluctance Motor
SRM	Switched Reluctance Motor
IM	Induction Motor
IPM	Interior Permanent Magnet
MOO	Multi-Objective Optimization
FEA/M	Finite Element Analysis/Method
SPM	Surface Permanent Magnet
NSGA	Non-dominated Sorting Genetic Algorithm
DOE	Design Of Experiment
GPR	Gaussian Process Regression
SVR	Support Vector Regression
ANN	Artificial Neural Network
MTPA	Maximum Torque Per Ampere
FOC	Field Oriented Control
CPSR	Constant Power Speed Range
RBF	Radial Basis Function
RMSE	Root Mean Squared Error
WLTP	Worldwide Harmonised Light Vehicle Test Procedure
EMF	Electromotive Force
MTPV	Maximum Torque Per Voltage
LHS	Latin Hypercube Sampling
EHVI	Expected Hypervolume Improvement
SAEO	Surrogate-assisted Evolutionary optimization
POF	Probability Of Feasibility
HVI	Hypervolume Improvement

Notation

V_{dc}	DC bus voltage
e_{ab}	Line-to-line induced back-EMF
P_e	Electromagnetic power
$P_{m,rated}$	Rated mechanical power
T_{rated}	Rated torque
N_{rated}	Rated speed
T_{pk}	Peak torque
$P_{m,pk}$	Peak mechanical power
N_{pk}	Peak speed
T_{ripple}	Torque ripple
I_{pk}	Peak phase current (rms)
L_{stk}	Active length of motor
r_{od}	Stator outer radius
r_{id}	Stator inner radius
w_t	Tooth thickness
h_{bi}	Yoke thickness
h_s	Slot height
g	Airgap length
τ_p	Rotor pole pitch
p	Pole pairs
τ_s	Stator slot pitch
τ_{pr}	Projection angle
τ_n	Notch angle
h_n	Notch depth
γ	Magnet V angle
b_1, b_2	Outer rib, Inner rib
λ_{pm}	permanent magnet (PM) flux linkage
L_q, L_d	Stator q- and d-axis inductances
i_q, i_d	q- and d-axis components of the stator phase current
ζ	Saliency ratio
β	Current phase angle
A_f	Frontal area
C_d	Drag coefficient
μ_{rr}	Rolling resistance coefficient
$\mathbf{x}$	k-vector of input design variables
$\mathbf{X}$	Sampling plan
$\mathbf{y}$	m-vector of output variables
$\mathbf{g}$	c-vector of constraints